

Literature Report

Reporter: 鲍鹏骏

Date: 2022-03-10



An Optical Probe for Real-Time Monitoring of Self-Replicator Emergence and Distinguishing between Replicators

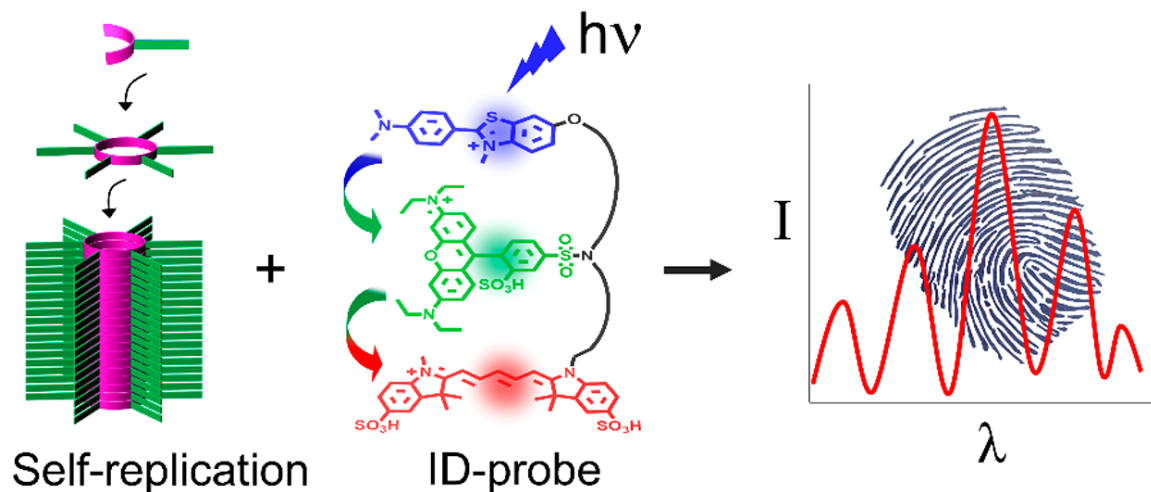
Joydev Hatai, Yigit Altay, Ankush Sood, Armin Kiani, Marcel J. Eleveld, Leila Motiei, David Margulies,* and Sijbren Otto*



Cite This: *J. Am. Chem. Soc.* 2022, 144, 3074–3082



Read Online



Literature Source



Sijbren Otto

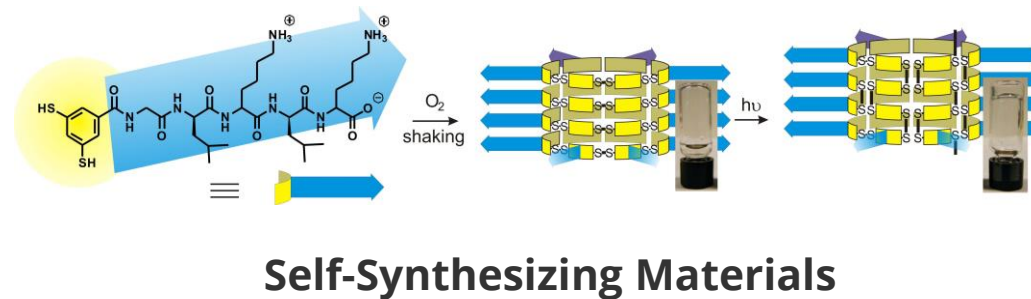
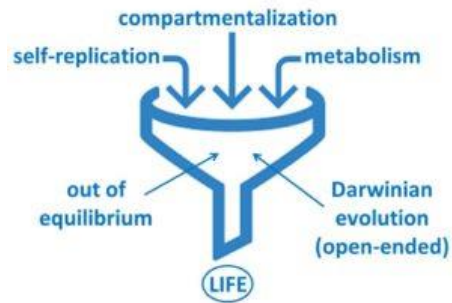
M.Sc. (1994) and Ph.D. (1998) from the University of Groningen in the Netherlands

1998 postdoctoral researcher in Lehigh University, Pennsylvania investigating synthetic systems mediating ion transport through lipid bilayers.

1999 University of Cambridge, UK, where he worked for two years on dynamic combinatorial libraries.

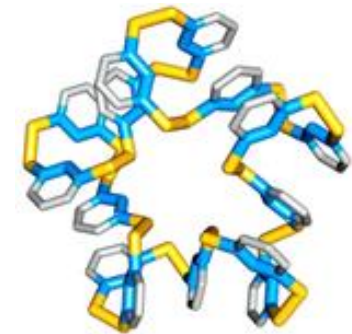
2001 as a Royal Society University Research Fellow at the University of Cambridge in the UK and accepted an appointment as Assistant Professor at the University of Groningen in 2009 and was promoted to Associate Professor in 2011 and Full Professor in 2016.

From self-replication towards de-novo life



Self-Synthesizing Materials

Self-synthesizing foldamer



Literature Source



David Margulies

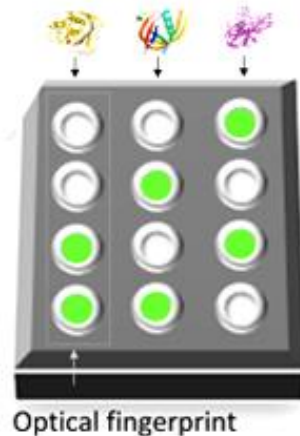
1998-2006 M.Sc., Ph.D., Weizmann Institute of Science – Israel, Department of Organic Chemistry.

2006–2009 Post-doctoral Associate, Yale University – USA, Department of Chemistry.

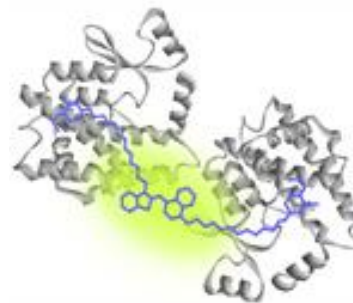
2009- 2017 Senior Scientist, Weizmann Institute of Science – Israel, Department of Organic Chemistry.

2017-present Associate Professor, Weizmann Institute of Science – Israel, Department of Organic Chemistry.

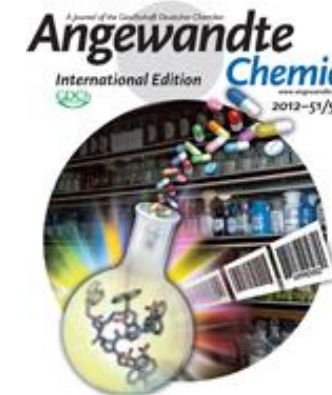
Cross-reactive sensor arrays



Combinatorial fluorescent molecular sensors



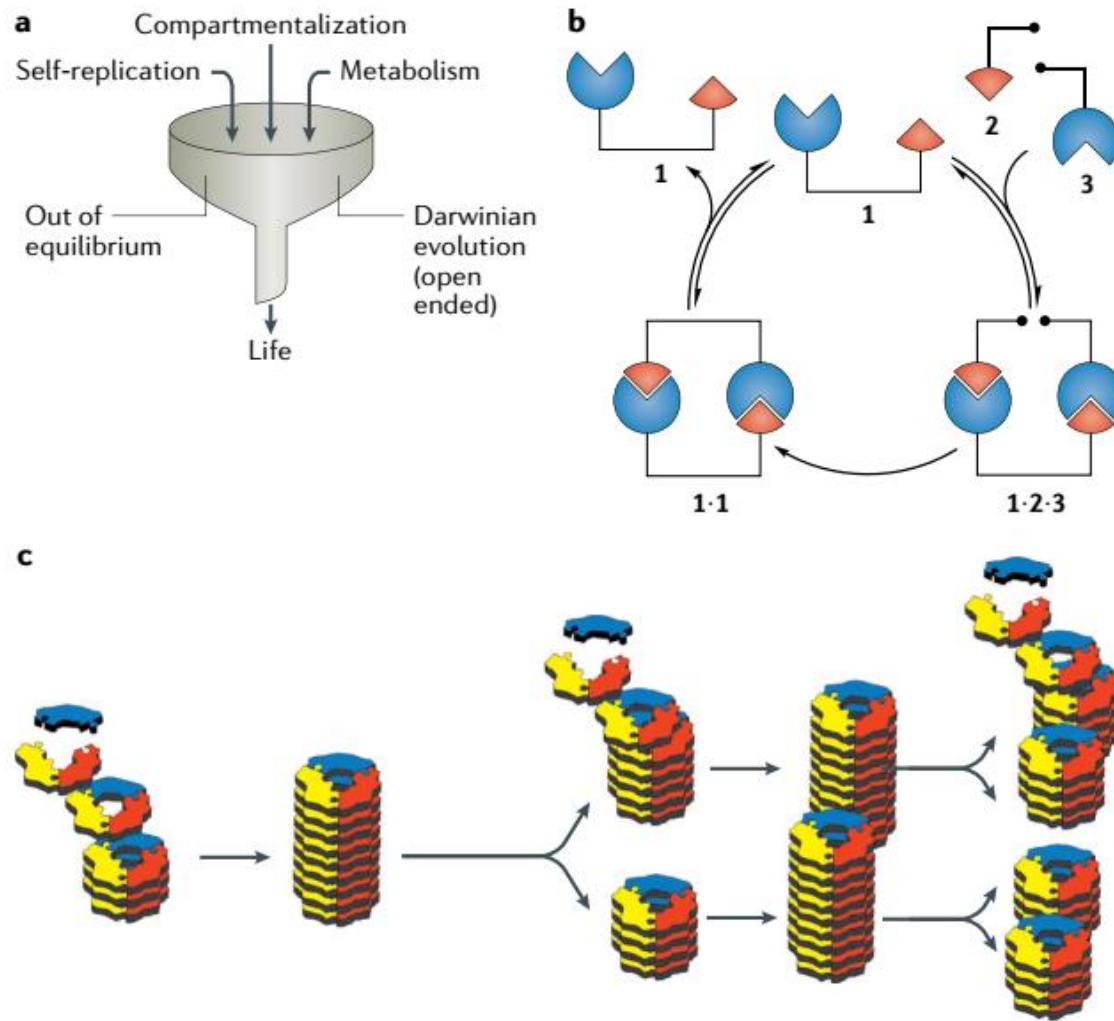
Fluorescent molecular sensors



Self-assembled biomimetics



Introduction



生命的基本特征和自我复制的主要机制

Result and Discussion



自我复制系统

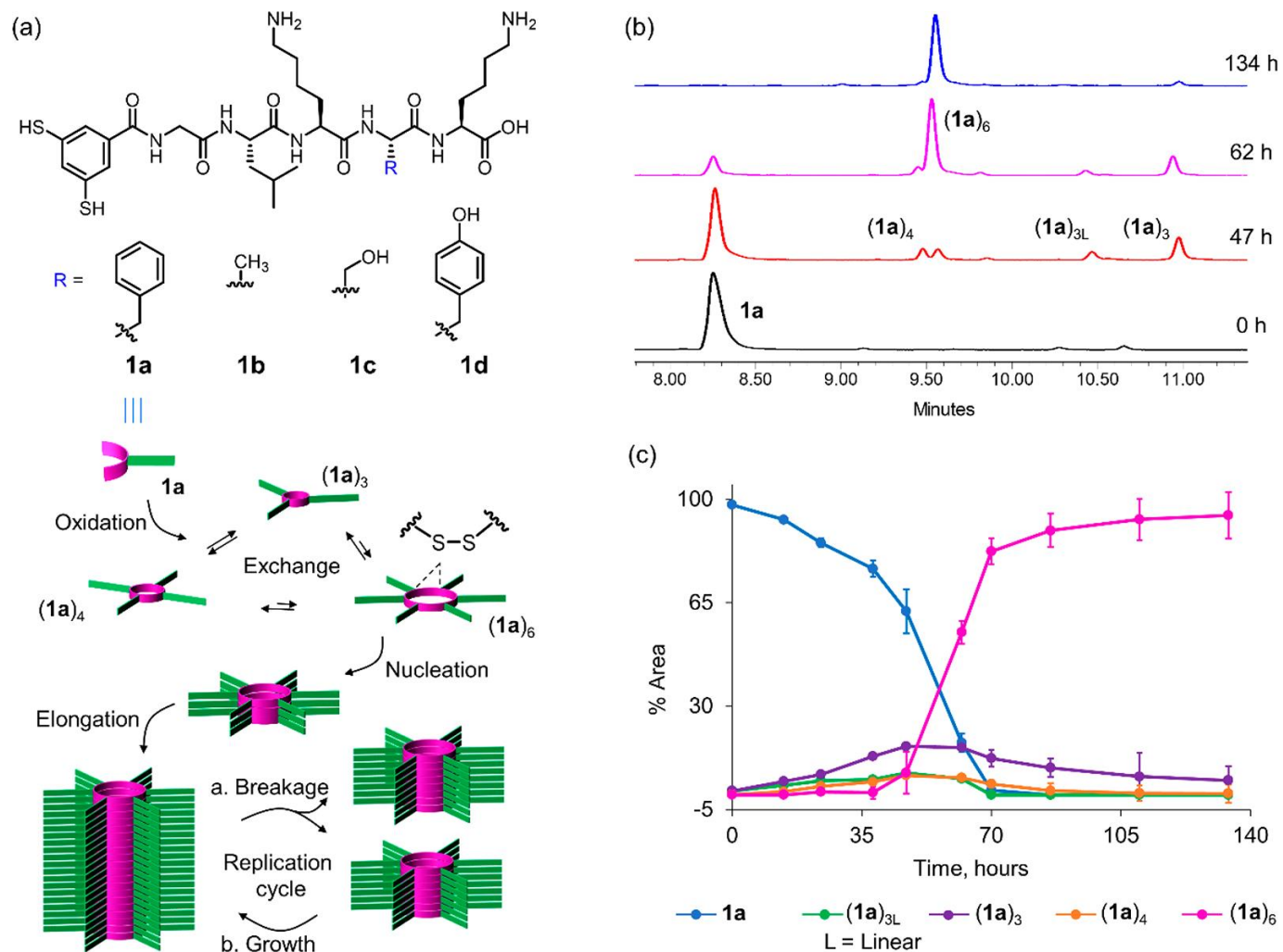


Figure 1. (a) Mechanism of self-assembly-driven self-replication. Air oxidation of dithiol building block **1a** initially produces a mixture of disulfide macrocycles of different ring sizes that interconvert through thiol–disulfide exchange. Assembly of, in this case, the cyclic hexamer $(1a)_6$ into fibers results in the autocatalytic production of more hexamer. Fiber formation is driven by a combination of π -stacking interactions and the assembly of the peptide tails into β -sheets. Agitation-induced fiber breakage liberates more growing fiber ends, enabling exponential growth. (b) Selected ultraperformance liquid chromatography (UPLC) traces (monitored at 254 nm) recorded at different stages during the emergence of replicator $(1a)_6$. (c) Kinetic profile (average of three independent experiments) of the emergence of $(1a)_6$. Samples were made from 30 μ M building block **1** in 50 mM (in boron atoms) borate buffer, pH 8.2, stirred at 1200 rpm at 30 °C

Result and Discussion



探针分子

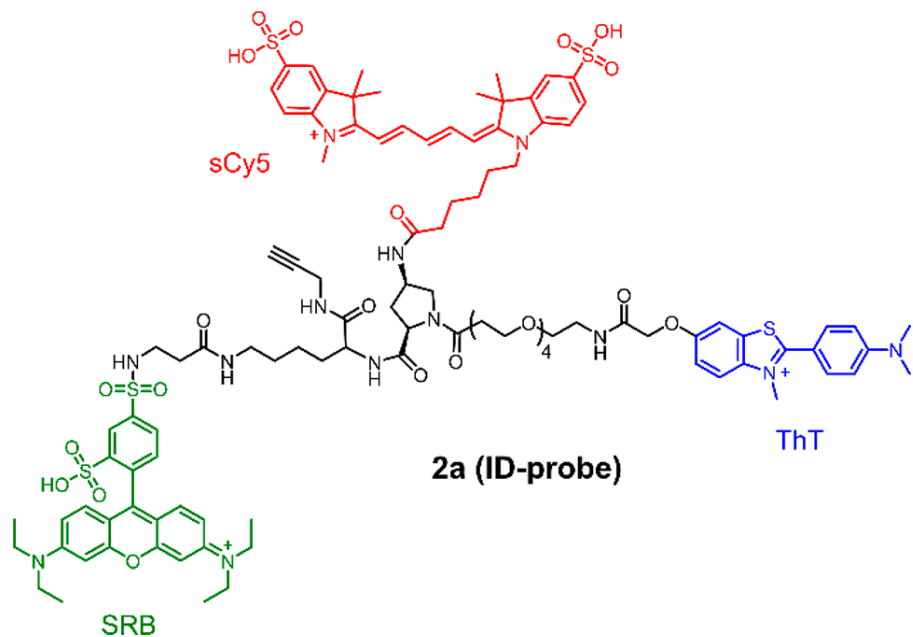


Figure 2. Structure of the pattern-generating ID-probe 2a carrying three fluorescent reporters: ThT (blue, Ex: 440 nm, Em: 490 nm), SRB (green, Ex: 530 nm, Em: 595 nm), and sCy5 (red, Ex: 630 nm, Em: 675 nm).

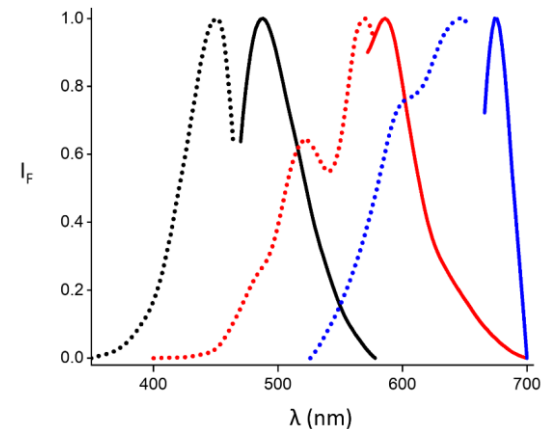


Figure S1. Normalized excitation (dotted line) and emission spectra (solid line) of ThT (with replicator fibers (1a)₆, black line), SRB (red line), and sCy5 (blue line)

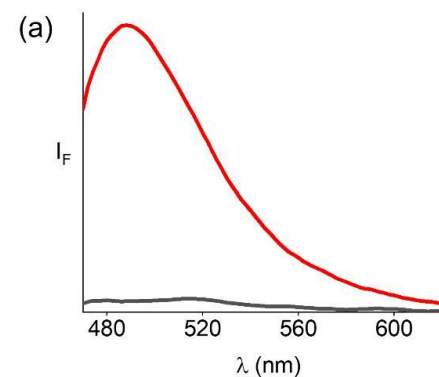


Figure S3. Emission spectra of ThT (2.0 μM, black line, 50 mM borate buffer) in the presence of fibers (1a)₆ (30 μM in building block 1a, red line);

Result and Discussion



ID-Probe 响应涉及 FRET

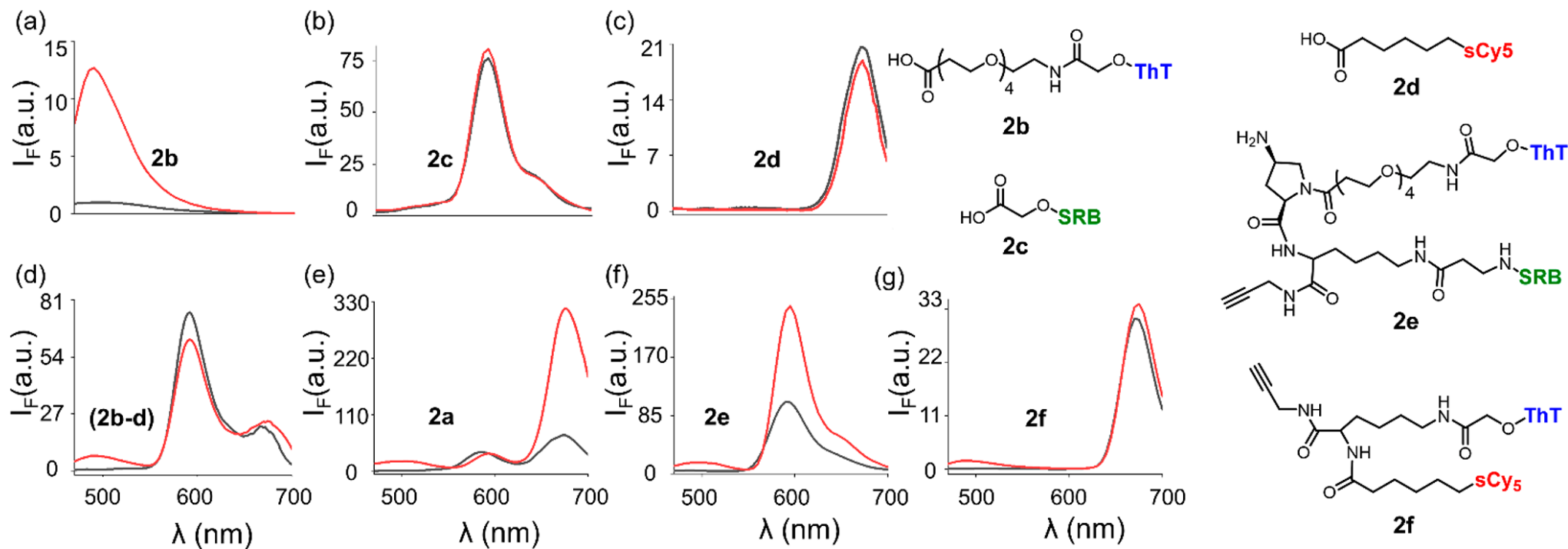


Figure 3. Emission spectra ($\lambda_{\text{ex}} = 440$ nm) of control molecules (a) 2b; (b) 2c; (c) 2d; and (d) an equimolar mixture of 2b, 2c, and 2d. Emission spectrum of (e) probe 2a and that of different binary dye conjugates (f) 2e and (g) 2f. Conditions: 2.0 μM dye construct(s), 50 mM borate buffer (pH 8.2), in the absence (black line) and presence (red line) of fibers of replicator (1a)₆ (30 μM in building block 1a). The fluorescence intensity shown on the y axes is normalized against the emission intensity of 2b at 490 nm in buffer

Result and Discussion



传感器可以区分不同的复制器及其前体

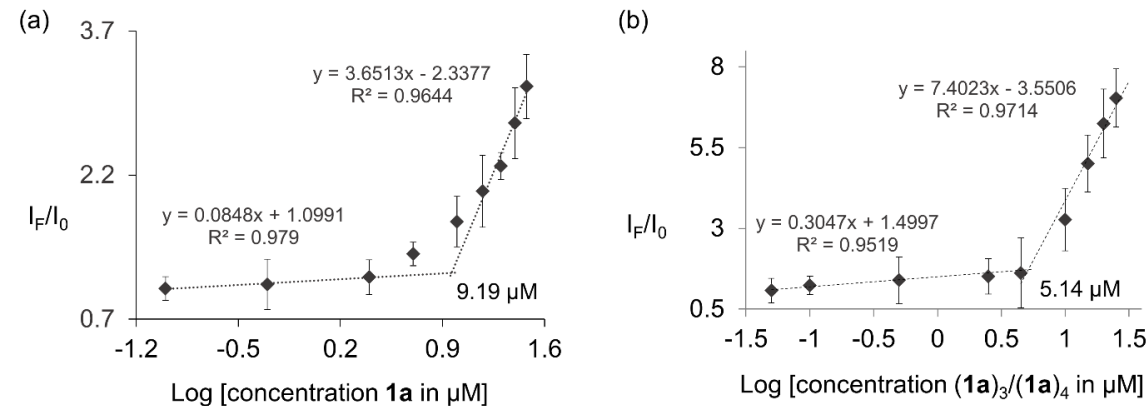
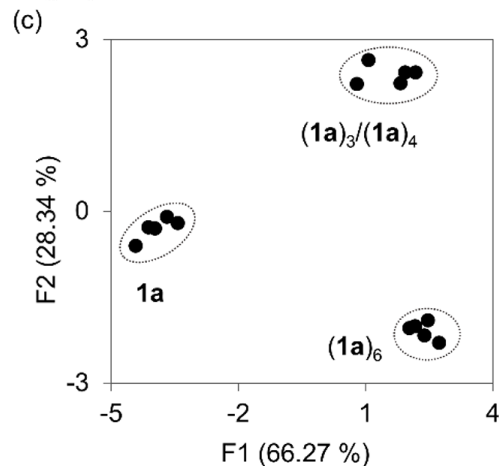
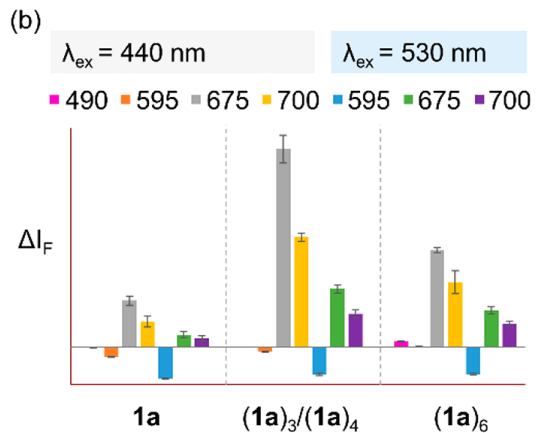
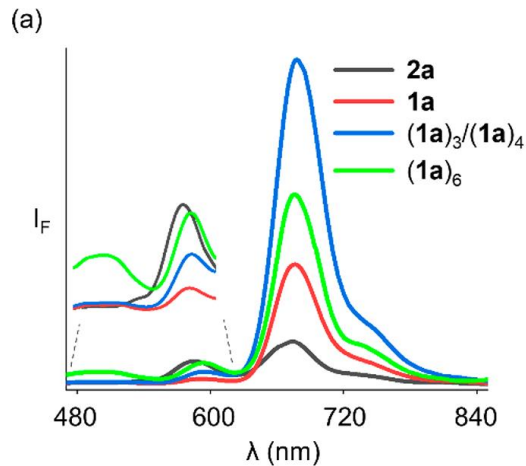


Figure S4. Determination of critical aggregation concentration (CAC) by titration 2a (2.0 μM , 50 mM borate buffer, pH 8.2) with different concentration of (a) monomers 1a, and (b) mixture of trimer and tetramer $(1a)_3/(1a)_4$ (50 mM borate buffer, pH 8.2). Concentrations are given in units of building block 1a.

PCA 是一种线性变换数据处理技术，通常用于降低多维数据集的维数，从而实现可视化。它选择数据的线性组合（主要成分；这里选择特定波长的荧光强度），使数据在二维图中的分布最大化。结果表明，2a 可以区分单体，三聚体/四聚体和由 1a 制成的纤维。

Figure 4. (a) Emission spectra of 2a (2.0 μM , 50 mM borate buffer, pH 8.2) in the presence of monomer 1a, a mixture of trimers and tetramers $(1a)_3/(1a)_4$, or replicator fibers $(1a)_6$, all at a concentration of 30 μM in units of 1a. (b) Change in fluorescence intensity of 2a at different emission channels ($\lambda_{\text{ex}} = 440$ and 530 nm, respectively) upon being exposed to 1a, $(1a)_3/(1a)_4$, or replicator fibers $(1a)_6$. (c) Principle component analysis (PCA) of the fluorescence data in (b) showing five repeats for each sample

Result and Discussion



传感器能够在原位监测自我复制器的形成

Table 1. Composition of Samples Prepared by Mixing Different Molar Ratios of Fibers $(1a)_6$ to Trimers–Tetramers $(1a)_3/(1a)_4$

sample	sample composition (%) ^a	
	trimers–tetramers $(1a)_3/(1a)_4$	fibers $(1a)_6$
1	100	0
2	80	20
3	60	40
4	30	70
5	0	100

^aThe total concentration of each sample was 30 μM in units of building block **1a**. These samples represent different stages of replicator emergence.

不同摩尔比表示复制的不同阶段

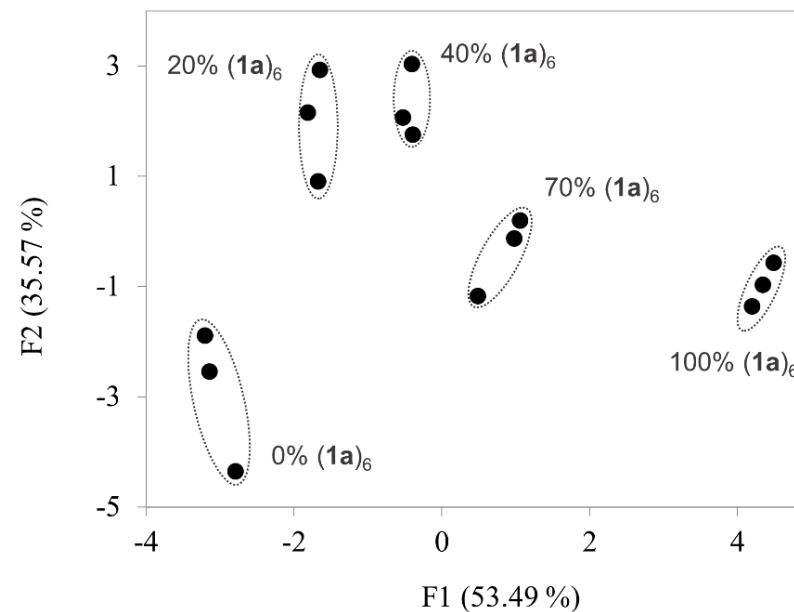


Figure S7. PCA of emission patterns ($\lambda_{\text{ex}} = 440 \text{ nm}$ and $\lambda_{\text{ex}} = 530 \text{ nm}$) obtained from the mixture of **2a** (2.0 μM) and the samples shown in Table 1 (main text)

PCA 表明探针2a可以区分不同摩尔比的前体和复制器

Result and Discussion



传感器能够在原位监测自我复制器的形成

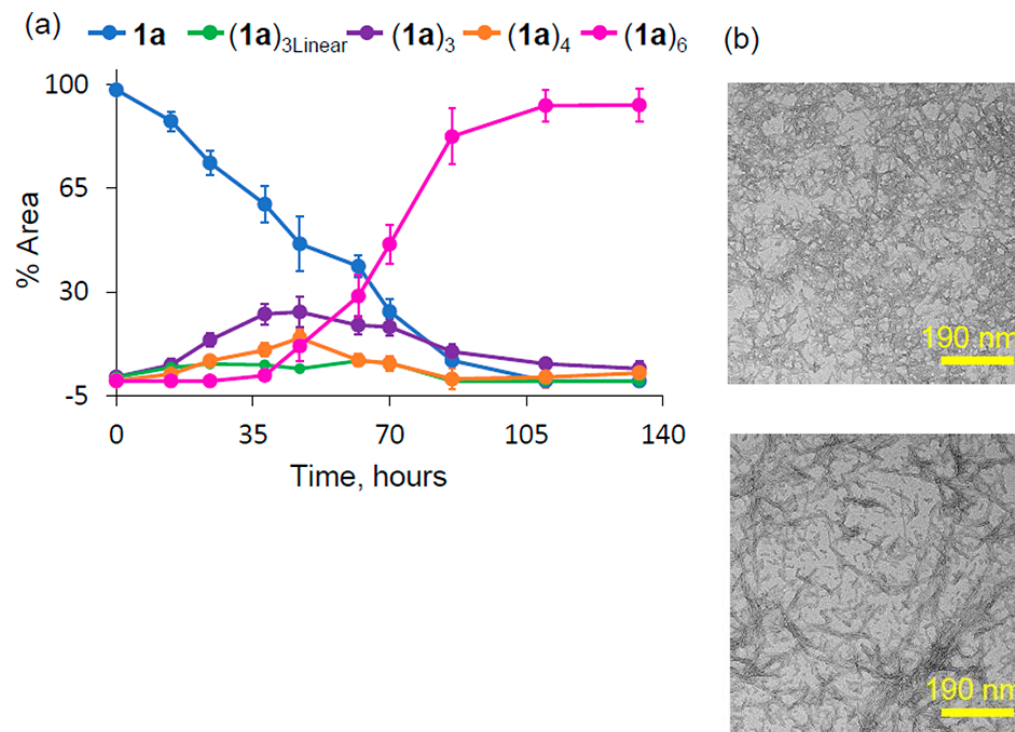


Figure 5. (a) UPLC analysis of the change in product distribution (average of three independent experiments) in a mixture made from building block 1a (30 μ M in building block 1a) co-incubated with sensor 2a (2.0 μ M) in borate buffer (50 mM, pH 8.2, stirred at 1200 rpm at 30 $^{\circ}$ C). (b) TEM images of fibers of replicator (1a)₆ in the absence (top) and presence (bottom) of sensor 2a.

探针的存在不影响混合物中不同复制子的动态形成

Result and Discussion



传感器能够在原位监测自我复制器的形成

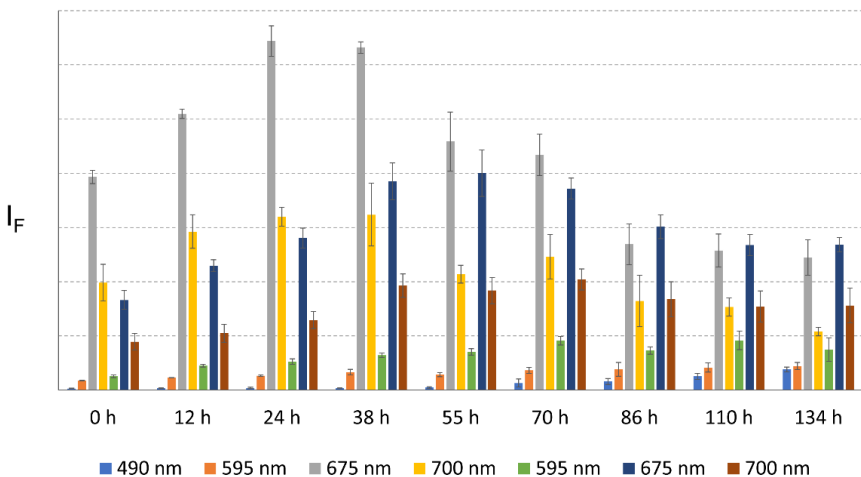
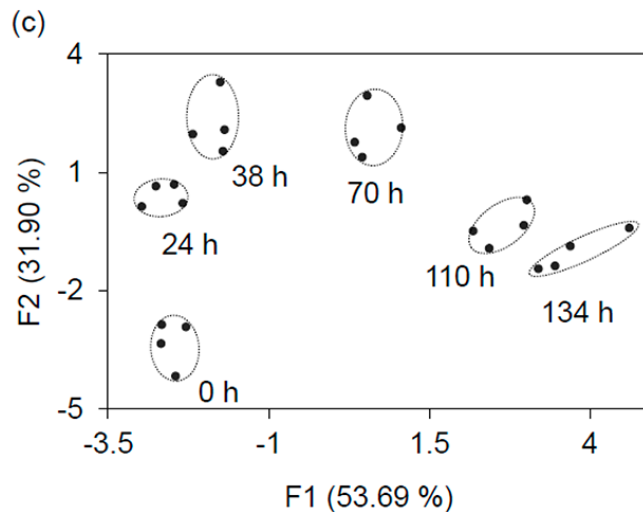


Figure S8. Change in fluorescence intensity of 2a at seven different emission channels ($\lambda_{ex} = 440$ nm and 530 nm, respectively) in a mixture made from building block 1a (30 μ M in building block 1a) coincubated with sensor 2a (2.0 μ M) in borate buffer (50 mM in boron atoms, pH 8.2, stirred at 1200 rpm at 30 $^{\circ}$ C



(c) PCA of the emission data recorded for the same sample at various time points.

对照实验:

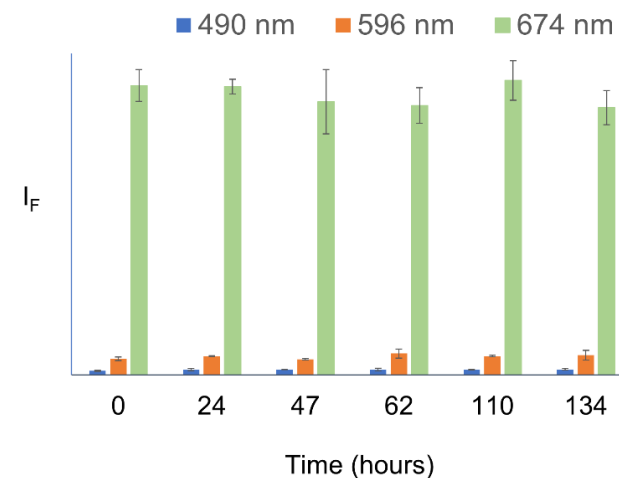


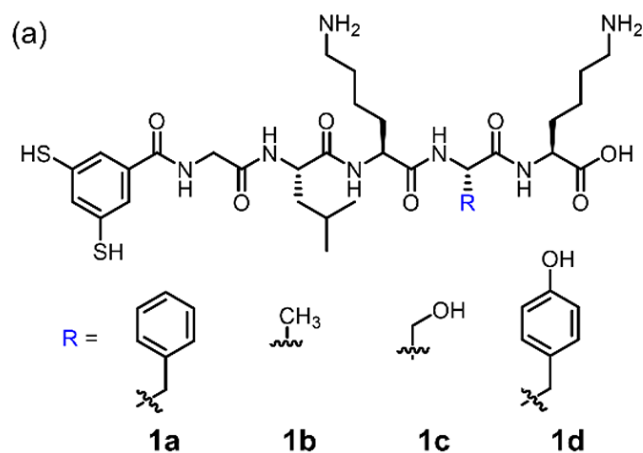
Figure S10. Emission of 2a (2.0 μ M) stirred at 1200 rpm in borate buffer (50 mM, pH 8.2) at 30 $^{\circ}$ C recorded at various time points. The emission of 2a did not change over time supporting the suitability of 2a for the real-time tracking of self-replicator.

探针可以在原位实时定性跟踪复制子的生长, 对照实验结果证实观察到的荧光变化是由混合物组成的变化引起的

Result and Discussion



可以区分不同的自我复制块



1a, 1b, 1c, 1d的分子结构

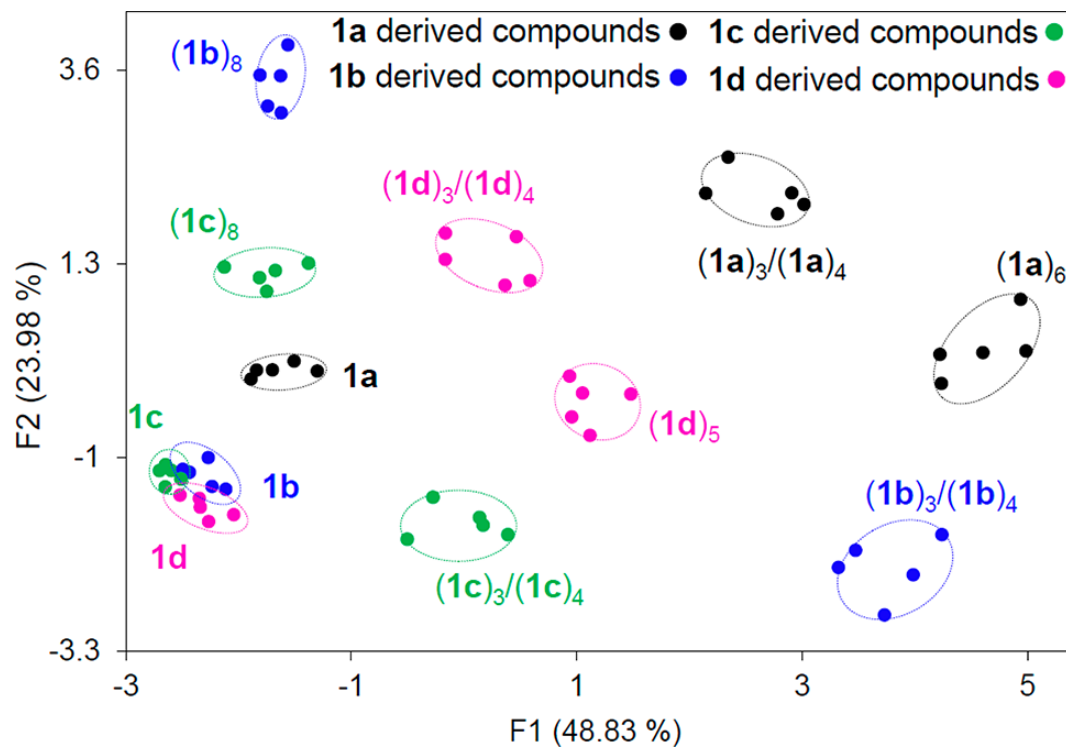


Figure 6. PCA of the emission patterns generated by 2a (2.0 μM) at different emission channels ($\lambda_{\text{ex}} = 440$ and 530 nm, respectively) in the presence of monomers, a mixture of trimers–tetramers, and replicator fibers prepared from building blocks 1a–d (30 μM in building block). The fluorescence data for each sample consist of five repeats.

PCA表明2a 可以区分不同大小的大环（三聚体和四聚体）和由不同构建块制成的复制器。然而，该探针难以区分构建这些系统的单体。